

DOI: 10.1002/ange.200501145

## Mechanism of the Initial Conformational Transition of a Photomodulable Peptide\*\*

Tadeusz Andruniów, Simona Fantacci,\*  
Filippo De Angelis, Nicolas Ferré, and  
Massimo Olivucci\*

The ability to control the specific conformation of peptides or proteins is highly desirable in the design of bioactive materials,<sup>[1]</sup> optical data storage devices,<sup>[2]</sup> or for triggering the folding/unfolding of oligopeptide chains.<sup>[3,4]</sup> Conformational changes in macromolecules can be achieved by incorporating a photoresponsive “monomer” into the molecule backbone;<sup>[5]</sup> such a monomer is capable of converting light energy into a permanent change in geometry. This approach is also seen in biological receptors<sup>[6–9]</sup> where the photoisomerization of organic chromophores is used to switch between different conformations. One of the most prominent examples of such switches is the protonated Schiff base (PSB) of retinal found in rhodopsin proteins. This chromophore undergoes a *cis*→*all-trans* photoisomerization that triggers a conformational change of the native protein scaffold.<sup>[10,11]</sup>

We recently concluded that synthetic PSBs may provide suitable frameworks for the design of molecular switches or motors.<sup>[12]</sup> We demonstrated that 5-methyl-4-(5'-methyl-

[\*] Dr. S. Fantacci, Dr. F. De Angelis  
Istituto CNR di Scienze e Tecnologie Molecolari (ISTM)  
c/o Dipartimento di Chimica  
Università degli Studi di Perugia  
via Elce di Sotto 8, 06123 Perugia (Italy)  
Fax: (+39) 075-585-5606  
E-mail: simona@thch.unipg.it

Dr. T. Andruniów, Prof. Dr. M. Olivucci  
Dipartimento di Chimica  
Università degli Studi di Siena  
via Aldo Moro, 53100 Siena (Italy)  
Fax: (+39) 0577-234-278  
E-mail: olivucci@unisi.it

Dr. T. Andruniów  
Institute of Physical and Theoretical Chemistry  
Department of Chemistry, Wrocław University of Technology  
Wyb. Wyspińskiego 27, 50-370 Wrocław (Poland)

Dr. N. Ferré  
Laboratoire de Chimie Théorique et de Modélisation Moléculaire  
UMR 6517-CNRS Universités Aix-Marseille  
Case 521, Centre de Saint-Jérôme  
13397 Marseille Cedex 20 (France)

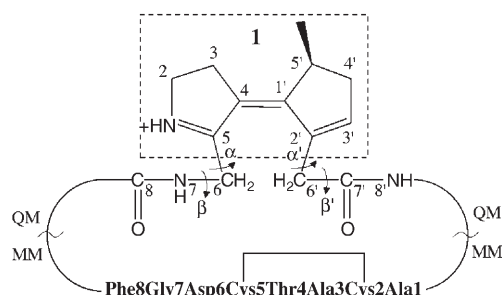
[\*\*] The authors are grateful to Prof. Peter Hamm, Dr. Jan Helbing, and Prof. Gerhard Stock for useful comments. This work was supported by the Università di Siena (PAR02/04), FIRB (RBAU01EPMR), and COFIN2004. M.O. and T.A. are grateful for a Marie-Curie grant (HPMF-CT-2002-01769).



Supporting information for this article (computational details, coordinates of all QM/MM and full QM optimized structures, tables of the energies and properties) is available on the WWW under <http://www.angewandte.org> or from the author.

cyclopent-2'-enylidene)-3,4-dihydro-2*H*-pyrrolinium, **1** in Scheme 1, a PSB featuring a “locked” backbone, satisfies the criteria for an efficient switch.

Previous studies on the octapeptide (**OP**) H<sub>2</sub>N-Ala1-Cys2-Ala3-Thr4-Cys5-Asp6-Gly7-Phe8-COOH, derived



**Scheme 1.** Subsystems of *cis*-**1-OP** treated by quantum mechanics (QM) and molecular mechanics (MM). Box (dotted lines) encloses **1**. Angles  $\alpha$ ,  $\beta$ ,  $\alpha'$ , and  $\beta'$  are discussed in the text.

from the thioredoxin reductase active site, revealed that this chain can be conveniently used to prepare a bicyclic peptide incorporating the azobenzene (Ab) photoisomerizable unit and a disulfide bridge.<sup>[7–9]</sup> In such a system light irradiation may be used to permanently switch the conformation of the peptide.

Herein, our target is to investigate the photoisomerization mechanism of an analogue system, **1-OP** in Scheme 1, where Ab is replaced with the computationally tractable<sup>[13]</sup> PSB unit **1**. While in previous studies,<sup>[3]</sup> which focused on longer timescales, the photochemical step was treated empirically, herein we show that the photoisomerization of *cis*-**1-OP** can be characterized by the novel quantum mechanics/molecular mechanics (QM/MM)<sup>[14,15]</sup> strategy recently applied to rhodopsin<sup>[16]</sup> and featuring a CASPT2//CASSCF QM level (see Experimental Section). To determine the intrinsic factors driving the transmission of the photoinduced strain to the peptide backbone we focus on gas-phase **1-OP**. The results indicate that while the switch starts to change immediately after excited state (*S*<sub>1</sub>) population, the change of the peptide moiety occurs only after decay to the ground state (*S*<sub>0</sub>). The resolution of the structure of the conical intersection funnel (CI) driving the *S*<sub>1</sub>→*S*<sub>0</sub> decay, allows the effect of the *S*<sub>0</sub> energy surface on the initial *S*<sub>0</sub> dynamics of **1-OP** to be explored. This effect is simulated at the QM level by running a 3 ps ground state Car–Parrinello<sup>[17]</sup> molecular dynamics (CPMD) trajectory.

Photoexcitation of *cis*-**1-OP** initiates the relaxation along the *S*<sub>1</sub> energy surface (Figure 1), ultimately leading to a CI located approximately 30 kcal mol<sup>−1</sup> lower in energy. The deformation driving the reactant out of the Franck–Condon (FC) region corresponds to a skeletal single-bond contraction and double-bond expansion (the reactive C4–C1' double bond is lengthened to 1.48 Å) coupled with an approximate 3° increase of the C5–C4–C1'–C2' torsion angle. Further evolution along the same coordinate, leads to a transition structure (TS<sub>ex</sub>) located about 4 kcal mol<sup>−1</sup> higher than *cis*-**1-OP**. Analysis of the TS<sub>ex</sub> structure indicates that the corresponding

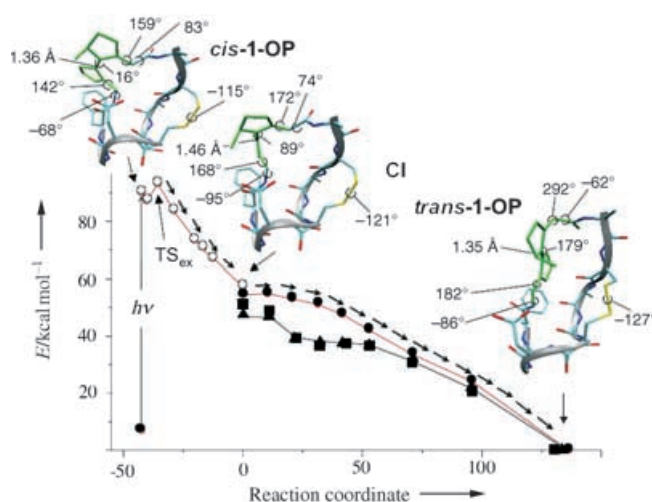


**Figure 1.** Energy profiles along the paths describing the *S*<sub>1</sub> and *S*<sub>0</sub> relaxation. The structures (geometrical parameters in [Å] and [°]) document the progression of the molecular structure of **1** and related link regions. The agreement between different computational methods is also shown (for computational details see Experimental Section and Supporting Information). ○ *S*<sub>1</sub> CASPT2//CASSCF/6-31G\*/Amber, ● *S*<sub>0</sub> CASPT2//CASSCF/6-31G\*/Amber, ■ PBE/6-31G\*, ▲ CP plane-wave PBE.

barrier is due to the steric repulsion between the hydrogen at C3 and methyl group at C5'. The steric repulsion is decreased by further twisting about the C4–C1' bond that drives the system along a barrierless region of the *S*<sub>1</sub> path. Along this region the stretching deformation of **1** decreases, the C4–C1' bond length stabilizes at 1.46 Å, and the twisting about this bond becomes dominant. The CI structure, located at the bottom of the *S*<sub>1</sub> surface, features a central double bond twisted by 89°.

Inspection of superimposed peptide backbones of the *cis*-**1-OP** and CI structures (Figure 2) reveals that, despite the difference in twist of unit **1** of approximately 75° in these two structures, the peptide conformations are still remarkably similar with a root-mean-square (rms) deviation of less than 0.6 Å. Both conformations exhibit a right-handed helical shape at Ala3 and an inverse  $\gamma$  turn centered on Asp6.

To provide mechanistic insight into the ground-state decay we have calculated the *S*<sub>0</sub> path departing from CI and leading to the photoproduct (*trans*-**1-OP**; Figure 1). The *S*<sub>0</sub> energy profile displays an approximately 0.9 kcal mol<sup>−1</sup> barrier at 102° twisting, suggesting the presence of a restrain force, attributed to initial peptide deformation. Further progression along the isomerization coordinate induces a limited change in energy up to 114° followed by a slope leading to the *trans*-**1-OP** energy minimum (characterized by a *trans* configuration of the switch).

Even though the superimposed peptide backbones of *cis*-**1-OP**, CI, and photoproduct structures share a common overall fold, *trans*-**1-OP** displays a more extended (stretched) conformation. Rms deviation between the CI and *trans*-**1-OP** peptide is about 1.5 Å. Analysis of the standard dihedral angles  $\phi$  and  $\psi$  along the backbone reveals that the helical character of Ala3 in the product is less pronounced than in the

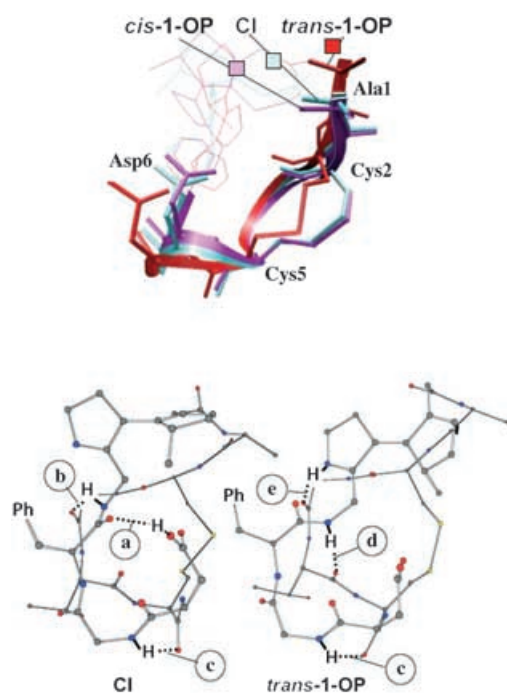


**Figure 2.** Top: superposition of the *cis*-1-OP (red), CI (blue), and *trans*-1-OP (magenta) structures. Bottom: hydrogen-bond patterns of CI and *trans*-1-OP. The hydrogen bonds a–e are discussed in the text.

reactant. However, *cis*- and *trans*-1-OP differ mainly in the orientation of the inner cycle formed by the disulfide bridge between Cys2 and Cys5. In fact, the limited twisting of the Cys2-S-S-Cys5 dihedral angle by about 25° is accompanied by the reorientation of residues Asp6, Gly7, and Phe8 of the C-terminal part of the peptide backbone.

The response of the peptide secondary structure to the isomerization of **1** is described in terms of the changes in the hydrogen-bond pattern (a–e, see Figure 2). The results suggest that on  $S_1$  there is no change in the number or location of the hydrogen bonds (three hydrogen bonds, indicated as a, b, and c in Figure 2, could be detected). However, upon departure from the CI structure and relaxation on the  $S_0$  energy surface, two new hydrogen bonds d and e that run between the Thr4 carbonyl group and the N7-H group of the link region and between the N<sup>+</sup>-H group of **1** and the Ala3 carbonyl group are formed. Similarly, the hydrogen bonds a and b between the Asp6 hydroxy and Phe8 carbonyl groups and between the N7-H of the link group and the Ala3 carbonyl, respectively, are broken. The only hydrogen bond that remains intact during both the  $S_0$  and  $S_1$  relaxations is c between the N-H group of Gly7 and the carbonyl group of Cys5. The treatment of the hydrogen bonds between atoms treated by QM and MM methods, has been validated by comparing the QM/MM and the full PBE-functional optimized structures of *cis*- and *trans*-1-OP. It is shown that by the QM/MM methods the hydrogen bonds a, b, and d are less than 0.04 Å longer at the PBE level. A larger difference is found for the bent hydrogen bond e that is 0.14 Å longer when computed at the PBE level.

The link regions between the switch **1** and the octapeptide are made up of the -CH<sub>2</sub>-NH- and -CH<sub>2</sub>-CO- groups

connected to carbon atoms C5 and C2', respectively (see Scheme 1). Accordingly, the evolution of these links is characterized in terms of the values of the angles  $\alpha$  (C4-C5-C6-N7) and  $\beta$  (C5-C6-N7-C8), and  $\alpha'$  (C1'-C2'-C6'-C7') and  $\beta'$  (C2'-C6'-C7'-N8'). It is apparent from Figure 1 that  $\alpha$  and  $\beta$  undergo a limited overall change (+40° and -18°) with respect to  $\alpha'$  and  $\beta'$  (+133° and -145°). Since, these changes provide information on the way the photoinduced torsional strain is transmitted from the switch to the octapeptide, we conclude that the strain is transmitted asymmetrically by the two link regions. This behavior is easily related to the fact that  $\alpha$  and  $\beta$  are made stiffer by the involvement of the N7-H, C8=O, and N<sup>+</sup>-H groups in the hydrogen-bond network. Notice that the change of  $\alpha'$  and  $\beta'$  along the  $S_1$  path is very limited. Thus, similar to the octapeptide chain, the link region changes mainly during  $S_0$  relaxation.

Information on the effect of the  $S_0$  path on the early  $S_0$  relaxation dynamics including the relative timescales of the leading molecular modes, are obtained through the analysis of a 3 ps CPMD trajectory. As shown in Figure 1, both CPMD (CP plane-wave PBE) and Gaussian98 PBE/6-31G\* yield energy profiles qualitatively close to the QM/MM one. The largest discrepancies are found in the initial part of the path where the density functional theory (DFT) curves show an inflection. The consistency of DFT//CASSCF and CASPT2//CASSCF  $S_0$  energy profiles for PSBs has been previously evaluated.<sup>[18]</sup> The relaxation process of the chromophore is monitored by the time evolution of the torsional deformation and length of the C4–C1' bond. The relaxation of the peptide is monitored by studying four hydrogen-bond lengths. Finally, the evolution of the link region between the switch and the peptide is studied by monitoring the  $\alpha'$  and  $\beta'$  angles.

As shown in Figure 3 the relaxation of the switch is characterized by coherent changes in torsional deformation

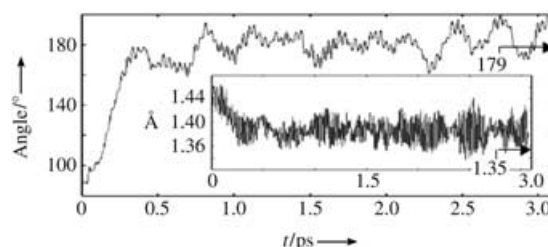


**Figure 3.** Time evolution of the C5-C4-C1'-C2' dihedral angle [°] and C4-C1' bond length [Å]. The arrows indicate the *trans*-1-OP values.

and bond lengths. In fact, both quantities approach the  $S_0$  equilibrium values in less than 0.5 ps. No back oscillation towards the  $S_1$  values is observed. On the other hand, the change in the peptide secondary structure reported in Figure 4 is consistent with a slower process (> 3 ps). In fact, although breaking of hydrogen bond a seems to occur on the picosecond timescale, a large oscillation is observed which continues up to 3 ps. An oscillatory behavior is also observed for the switching in the hydrogen bonds b and d. After 1 ps b is broken while d is formed. However, after 2 ps these hydrogen bonds are pushed back to their original positions, while at 2.5 ps a new inversion takes place. Remarkably, after 3.0 ps a,

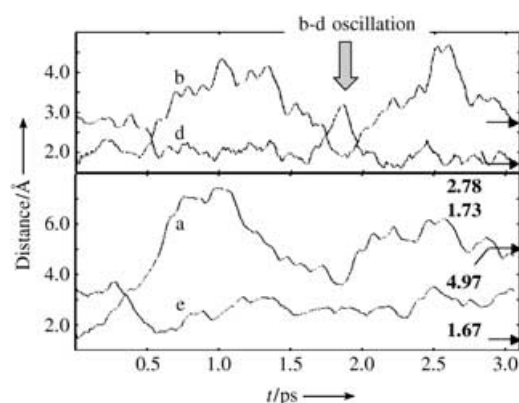


**Figure 4.** Evolution of the hydrogen bonds a, b, d, and e defined in Figure 2. The arrows indicate the *trans*-1-OP values.

b, and d seem to have reached the final values of the  $S_0$  *trans*-1-OP energy minimum. The behavior of hydrogen bond e is different. Although initial relaxation promotes formation of this (looser and bent) hydrogen bond just after 0.6 ps, the bond breaks and remains substantially broken up to the end of the simulation. This bond will require a longer time to reach the predicted equilibrium value. A behavior that can be associated to the bent geometry of e that features a N–H···O angle of 132°.

The dynamics of the link region is displayed in Figure 5. There is a high correlation between angles  $\alpha'$  and  $\beta'$  all along

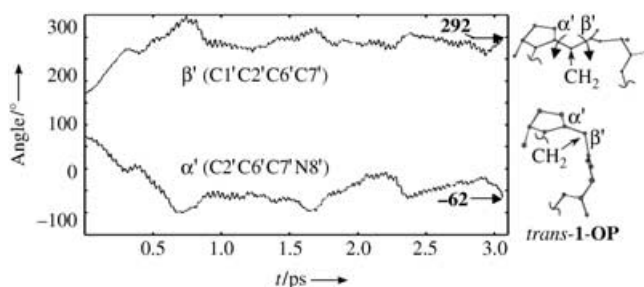


**Figure 5.** Time evolution of the link-region torsional angles  $\alpha'$  and  $\beta'$ . The arrows indicate the *trans*-1-OP values.

the simulation. They move according to a hula-twist motion (a clockwise and counterclockwise twist about two adjacent bonds) of the  $-\text{CH}_2-$  unit of the link. This movement provides a way to efficiently bend the linkage without introducing angular strain. The *trans*-1-OP product values are reached in less than 1 ps.

In conclusion, we describe the mechanism of photo-induced strain transmission in a naked macrocyclic cation. (Of course, owing to its effect on the hydrogen-bond stability and formation, a protic solvent may substantially change the mechanism and timescale of the relaxation. Solvent and counterion effects on 1-OP are currently under investigation). While the photoinduced conformational transition from *cis*-1-OP to *trans*-1-OP involves a total rms deviation of 2.0 Å, only a fraction of this change occurs during the  $S_1$  evolution, which mainly features stretching relaxation and an approximately

90° twisting of the switch unit 1. The documented  $S_1$  relaxation path indicates an ultrafast  $S_1 \rightarrow S_0$  decay dynamic at room temperature. In fact, 1) there is only a small barrier restraining the  $S_1$  evolution and 2) a  $S_1/S_0$  conical intersection provides a fully efficient  $S_1 \rightarrow S_0$  decay channel. These conclusions are consistent with the behavior observed for experimentally accessible Ab-peptide analogues<sup>[3,9]</sup> where decay to  $S_0$  occurs in under 1 ps. Our reaction path and trajectory analysis indicate that the peptide relaxation occurs entirely on  $S_0$  on a much longer timescale. Indeed, while the relaxation of the switch is substantially completed within 0.5 ps, the hydrogen bonds b, d, and e oscillate even after 2 ps with e still broken after 3 ps. On the other hand, the asymmetric relaxation of the link regions is found to occur on an intermediate time scale ( $< 1$  ps) indicating a sequential (switch  $\rightarrow$  link  $\rightarrow$  peptide) mechanism for the transmission of the strain generated by the switch. Loosely, these results are consistent with ultrafast IR spectroscopy measurements on an Ab-peptide analogue indicating that the photoinduced peptide stretching dynamics (that is associated with the redistribution of the strain) is completed in a time window between 6 and 20 ps.<sup>[9]</sup> Finally, notice that within the first half-oscillation in Figure 4, the backbone changes described by the trajectory and  $S_0$  relaxation path of Figure 1 (i.e. the static minimum energy path) are similar. Indeed, a transient geometry close to *trans*-1-OP is generated and lost after 0.7 ps indicating that the path accelerates the system directly towards the product structure.

## Experimental Section

**Computational Details:** Our QM/MM implementation is based on a hydrogen link-atom scheme with the frontier placed at the CO– $\text{C}_\alpha\text{H}$  and NH– $\text{C}_\alpha\text{H}$  bonds of Ala1 and Phe8, respectively (see Scheme 1). The ab initio QM calculations are based on a CASSCF/6-31G\* level. The active space comprises the full  $\pi$  system of 1 (six electrons in six  $\pi$  orbitals). For the MM part we use the Amber force field<sup>[19]</sup> with standard or re-parameterized van der Waals potentials. CASSCF/6-31G\*/Amber geometry optimizations are carried out with the GAUSSIAN98<sup>[20]</sup> (G98) and TINKER<sup>[21]</sup> programs. To account for dynamic electron correlation effects, re-evaluation of the energy of the optimized structures was carried out at the multiconfigurational second-order perturbation theory level using the CASPT2 implementation of MOLCAS-5<sup>[22]</sup> and a two-root state-averaged CASSCF zeroth-order wavefunction (CASPT2//CASSCF/6-31G\*/Amber level). The initial relaxation direction (IRD) method<sup>[23]</sup> was used to locate the steepest-descent direction to be followed when computing the  $S_1$  (starting at *cis*-1-OP) and  $S_0$  (starting at CI) branches of the reaction path of Figure 1. To simulate the  $S_0$  relaxation dynamics a single CPMD trajectory starting at CI with zero initial velocities (the sensitivity of the trajectory to a random distribution of velocities at CI has been tested.  $\alpha'$  and  $\beta'$  are found to be the most sensitive variables) was calculated at the full QM level, using the PBE exchange-correlation functional<sup>[24]</sup> with a plane-wave basis set and ultrasoft pseudopotentials.<sup>[25,26]</sup> Additional single-point CPMD and G98 PBE/6-31G\* calculations were performed on the QM/MM  $S_0$  branch to check the consistency of DFT and QM/MM results. See Supporting Information for further computational details.

Received: March 31, 2005

Revised: May 6, 2005

Published online: August 18, 2005



**Keywords:** ab initio calculations · molecular switches · peptides · photochemistry · reaction mechanisms

- [1] a) V. J. Hruby, J.-M. Ahn, S. Liao, *Curr. Opin. Chem. Biol.* **1997**, *1*, 114–119; b) A. S. Ripka, D. H. Rich, *Curr. Opin. Chem. Biol.* **1998**, *2*, 441–452.
- [2] a) B. L. Feringa, W. F. Jager, B. De Lange, *Tetrahedron* **1993**, *49*, 8267–8310; b) P.-O. Astrand, P. S. Ramanujam, S. Hvilsted, K. L. Bak, S. P. A. Sauer, *J. Am. Chem. Soc.* **2000**, *122*, 3482–3487.
- [3] S. Spörlein, H. Carstens, H. Satzger, C. Renner, R. Behrendt, L. Moroder, T. Tavan, W. Zinth, J. Wachtveitl, *Proc. Natl. Acad. Sci. USA* **2002**, *99*, 7998–8002.
- [4] V. Kräutler, A. Aemissegger, P. H. Hünenberger, D. Hilvert, T. Hansson, W. F. van Gunsteren, *J. Am. Chem. Soc.* **2005**, *127*, 4935–4942.
- [5] a) I. Willner, S. Rubin, *Angew. Chem.* **1996**, *108*, 419–439; *Angew. Chem. Int. Ed. Engl.* **1996**, *35*, 367–385; b) I. Willner, *Acc. Chem. Res.* **1997**, *30*, 347–356.
- [6] L. Ulysse, J. Cubillos, J. Chmielewski, *J. Am. Chem. Soc.* **1995**, *117*, 8466–8467.
- [7] R. Behrendt, C. Renner, M. Schenk, F. Wang, J. Wachtveitl, D. Oesterheld, L. Moroder, *Angew. Chem.* **1999**, *111*, 2941–2943; *Angew. Chem. Int. Ed.* **1999**, *38*, 2771–2774.
- [8] C. Renner, R. Behrendt, S. Spörlein, J. Wachtveitl, L. Moroder, *Biopolymers* **2000**, *54*, 489–500.
- [9] J. Bredenbeck, J. Helbing, A. Sieg, T. Schrader, W. Zinth, C. Renner, R. Behrendt, L. Moroder, J. Wachtveitl, P. Hamm, *Proc. Natl. Acad. Sci. USA* **2003**, *100*, 6452–6457.
- [10] R. A. Mathies, J. Lugtenburg In *Handbook of Biological Physics*, Vol. 3 (Eds.: D. G. Stavanga, W. J. de Grip, E. N. Pugh), Elsevier Science B.V., Dordrecht, **2000**, pp. 56–90.
- [11] H. Kandori, Y. Shichida, T. Yoshizawa, *Biochemistry (Moscow)* **2001**, *66*, 1583–1598.
- [12] D. Sampedro, A. Migani, A. Pepi, E. Busi, R. Basosi, L. Latterini, F. Elisei, S. Fusi, F. Ponticelli, V. Zanirato, M. Olivucci, *J. Am. Chem. Soc.* **2004**, *126*, 9349–9359.
- [13] The reactivity of the Ab chromophore is presently untractable at the CASSCF level used herein. This problem is mainly due to the large active space required (18 electrons in 16 orbitals).
- [14] A. Warshel, M. Levitt, *J. Mol. Biol.* **1976**, *103*, 227–249.
- [15] M. J. Field, P. A. Bash, M. Karplus, *J. Comput. Chem.* **1990**, *11*, 700–733.
- [16] T. Andrúniów, N. Ferré, M. Olivucci, *Proc. Natl. Acad. Sci. USA* **2004**, *101*, 17908–17913.
- [17] R. Car, M. Parrinello, *Phys. Rev. Lett.* **1985**, *55*, 2471–2474.
- [18] S. Fantacci, A. Migani, M. Olivucci, *J. Phys. Chem. A* **2004**, *108*, 1208–1213.
- [19] P. A. Kollman, R. Dixon, W. Cornell, T. Fox, C. Chipot, A. Pohorille in *Computer Simulation of Biomolecular Systems*, Vol. 3 (Eds.: A. Wilkinson, P. Weiner, W. F. Gunsteren), Elsevier, Dordrecht, **1997**, pp. 83–96.
- [20] Gaussian 98 (Revision A.7), M. J. Frisch, G. W. Trucks, H. B. Schlegel, G. E. Scuseria, M. A. Robb, J. R. Cheeseman, V. G. Zakrzewski, J. A. Montgomery, R. E. Stratmann, J. C. Burant, S. Dapprich, J. M. Millam, A. D. Daniels, K. N. Kudin, M. C. Strain, O. Farkas, J. Tomasi, V. Barone, M. Cossi, R. Cammi, B. Mennucci, C. Pomelli, C. Adamo, S. Clifford, J. Ochterski, G. A. Petersson, P. Y. Ayala, Q. Cui, K. Morokuma, D. K. Malick, A. D. Rabuck, K. Raghavachari, J. B. Foresman, J. Cioslowski, J. V. Ortiz, B. B. Stefanov, G. Liu, A. Liashenko, P. Piskorz, I. Komaromi, R. Gomperts, R. L. Martin, D. J. Fox, T. Keith, M. A. Al-Laham, C. Y. Peng, A. Nanayakkara, C. Gonzalez, M. Challacombe, P. M. W. Gill, B. G. Johnson, W. Chen, M. W. Wong, J. L. Andres, M. Head-Gordon, E. S. Replogle, J. A. Pople, Gaussian, Inc., Pittsburgh, PA, **1998**.
- [21] J. W. Ponder, F. M. Richards, *J. Comput. Chem.* **1987**, *8*, 1016–1024.
- [22] K. Andersson, M. R. A. Blomberg, M. P. Fülscher, G. Karlström, R. Lundh, P.-A. Malmqvist, P. Neogrády, J. Olsen, B. O. Roos, A. J. Sadlej, M. Schütz, L. Seijo, L. Serrano-Andrés, P. E. M. Siegbahn, P.-O. Widmark, University of Lund, Lund, Sweden, **2002**.
- [23] O. Celani, M. A. Robb, M. Garavelli, F. Bernardi, M. Olivucci, *Chem. Phys. Lett.* **1995**, *243*, 1–8.
- [24] J. P. Perdew, K. Burke, M. Ernzerhof, *Phys. Rev. Lett.* **1996**, *77*, 3865–3868.
- [25] A. Pasquarello, K. Laasonen, R. Car, C. Lee, D. Vanderbilt, *Phys. Rev. Lett.* **1992**, *69*, 1982–1985.
- [26] P. Giannozzi, F. De Angelis, R. Car, *J. Chem. Phys.* **2004**, *120*, 5903–5915.